SENSITIVITY OF MELT POOL SIZE AND POROSITY APPEARING TO BASE PLATE PREHEATING IN LASER POWDER BED FUSION PROCESS

N. Hassine[1], S. Chatti[1*], L. Kolsi[2,3]

[1]Laboratory of Mechanical Engineering, National Engineering School of Monastir, University of Monastir, Rue Ibn El Jazzar, 5000 Monastir, Tunisia
[2]Department of Mechanical Engineering, College of Engineering, University of Ha'il, Ha'il City 81451, Saudi Arabia
[3]Laboratory of Metrology and Energy Systems, Department of Energy Engineering, University of Monastir, 5000 Monastir, Tunisia
*Corresponding author's e-mail address: sami.chatti@udo.edu

ABSTRACT

The base plate temperature ranks among the crucial building parameters whose effect on melt pool dimensions and porosity defects generation has not been sufficiently discussed in literature. In the current study, with the aim to explore the dependence between melt pool dimensions, porosity defects and base plate preheating, a 3-dimensional thermal finite element model is carried out to create IN718 single beads, at various base plate temperatures. The dimensions of the melt pool behave favourably with the base plate preheating. Indeed, the melt pool depth, width and length increase continuously with the heat of the base plate, from 20 °C to 500 °C. The melt pool width is more responsive to the base plate temperature than the melt pool depth. Numerical results also indicate that the melt dimensions become more responsive to the temperature of the base plate at a slower scan speed. The degree of porosity is predicted under multiple values of base plate temperature and the results show that porosity tends to disappear with further preheating of the base plate. A satisfying accordance between the numerical finding and the experimental results from literature is identified.

KEYWORDS: Laser powder bed fusion, base plate preheating, melt pool size, porosity defects, single bead.

1. INTRODUCTION

Laser powder bed fusion (LPBF), as a promising metal additive manufacturing technique [17], is applied to manufacture, in an upwards manner, layer by layer complex 3D components. The process consists of melting thin layers of metallic powder along a specific path using the laser as a heat source [27]. Thanks to the multilayered character of the process, a variety of complex parts can be fabricated [24].

The LPBF process is widely adopted in various industrial applications such as medical implants and aeronautic components [22], since it ensures 3D parts with higher performance than that of traditional processes (Fig. 1).

Nevertheless, LPBF presents some drawbacks related to the final part quality. In fact, the multiple thermal cycles, i.e., the rapid heating and cooling material cycles significantly reflect the 3D part quality. The effect of machine input parameters including layer thickness, scan speed, laser spot size, and laser power

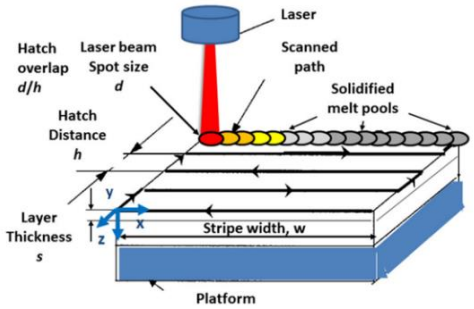

Fig. 1. Schematic representing the LPBF process **[**7]

are the majority issues treated in literature. Indeed, Choo et al. [6] explored the relationship between laser power and the defects characteristics of 316L stainless 3D parts. Recently, the impact of laser beam diameter on melt pool sizes and porosity defects generation was investigated, and the results revealed that there is a meaningful relation between the spot size and the defects appearing [10]. Furthermore, the impact of the

https://doi.org/10.35219/awet.2022.11
Date of submission/acceptance: 01.10.2022/15.12.2022

hatch spacing on melt pool sizes and porosity defects generation was studied, and the finding revealed that there is a meaningful dependence between the hatch spacing and the defects appearing [8], [9]. The relationship between porosity and mechanical properties was also studied by various researchers. They found that the porosity degrades the mechanical properties [12], [13] and, thus, limits the lifetime of a product [20].

The impact of powder layer thickness has been discussed. In fact, Leitch et al. [16] demonstrated that increasing the layer thickness is beneficial in terms of faster productivity, however, lack of fusion defect is registered with high layer thickness. The same finding is proved by [21]. The effect of laser power and scan speed on the melt pool morphology and the porosity development has been widely addressed in literature. Most of the research proves that both parameters significantly affect the final part's quality. Indeed, an increase in the scan speed accompanied by low laser power generally leads to a lack of fusion defect [23].

Yet, another process parameter, which is equally as relevant as the other ones, is the base plate temperature. Preheating, i.e. increasing the base plate temperature, is considered to be one of the techniques that enhance parts quality.

The temperature of the base plate is also a critical parameter, influencing the properties of the material. In fact, in the investigation mentioned in [3], when the preheating temperature is equal to 250 °C, part distortion becomes irrelevant.

Furthermore, preheating the base plate may avoid cracking and delamination due to residual stress [14]. A considerable improvement in yield strength and ductility and in the Ti-6Al-4V 3D parts when the base plate temperature is set at 570 °C was noted in the research of Ali et al. [1].

The main incentive to use such method of preheating is the potential mitigation of thermal stresses. These facts were proved by Vrancken et al. They achieved in their investigation a significant reduction in residual stress of about 50% for the Ti-6Al-4V alloy, by applying a 400°C preheating temperature [25].

Nevertheless, further research noted some confusions when preheating the base plate. Actually, an increase in the residual stress is registered in [19], while others stated that the properties of the unmelted powder altered and, therefore, restricted its recycling [18]. Thus, it should be carefully selected. The preheating temperature depends on the type of material and requires an accurate setting.

Until now, the base plate preheating effects on melt pool dimensions and porosity defects generation have not been investigated in depth, and most of the available research is focusing on the relationship between base plate preheating, residual stress, and mechanical properties. To fill in this gap, our study presents a helpful tool to predict the effect of the base plate preheating at various temperatures on the melt pool dimensions and the porosity level. We believe that this work is needed to explore these issues and provide process recommendations to control the porosity defects that occur in 3D parts.

So far, the monitoring of part defects is a challenging task regarding the rapidity of the process and the inappropriate measuring methods during the process. Thus, computational models may be utilized to both predict such phenomena and offer useful guidance for process optimization.

2. MATERIALS AND METHODS

A 3D transient thermal finite element (FE) model was created to build a series of Inconel718 single beads deposited on the base plate. Figure 2 represents a schematic illustration showing the single bead on the base plate that will be preheated at various temperatures. It also shows the inputs of our model, including laser power, scan speed, and powder layer thickness. The powder is assumed to be a homogenous and absorbing medium. The outputs provided by Ansys, including the dimensions of the melt pool (depth, width, length), are also presented. What is more, the single bead is considered to be the basic unit of building, which strongly affects the quality of the final part. The melt pool dimensions, including depth, width and length, were evaluated at a large range of preheating temperatures of the base plate. The values of the latter vary from 100 °C to 500 °C which represent the upper value allowed in the used software program Ansys Additive. The value of 20 °C, which represents the minimum temperature in Ansys, is also tested. The building parameters, including laser power, were kept constant in all the cases, at a value of 285 W, in order to meet the experimental values. Concerning the scanning speed, it altered from 500 mm/s to 1500 mm/s, aiming to understand how the melt pool dimensions behave when preheating the base plate at various scan speed values.

The bulk quantity of the laser energy is absorbed by the powder particles and then dissipated through thermal conduction, which is governed by the following Fourier's equation. The temperature distribution can be determined from this equation [11]:

$$\rho c \frac{\partial T}{\partial t} = \frac{\partial}{\partial x}\left(k \frac{\partial T}{\partial x}\right) + \frac{\partial}{\partial y}\left(k \frac{\partial T}{\partial y}\right) + \frac{\partial}{\partial z}\left(k \frac{\partial T}{\partial z}\right) + Q \quad (1)$$

Where T, Q, k, ρ and c denote the temperature, the heat source input, the thermal conductivity, the material density, and the specific heat capacity, respectively, t and (x, y, z) are the time of interaction and the spatial coordinates.

The moving laser heat source follows a Gaussian distribution, where the heat flux density decreases exponentially away from the center, which can be mathematically defined by the following equation [15]:

$$Q = 2\frac{AP}{\pi W^2}\, exp\frac{-2r^2}{w^2} \quad (2)$$

where Q, P, A, w are the input heat flux, laser power, laser beam absorptivity, radius of the laser spot respectively, and r is the position from the laser point center, at a specific time t, to a point on the powder bed surface.

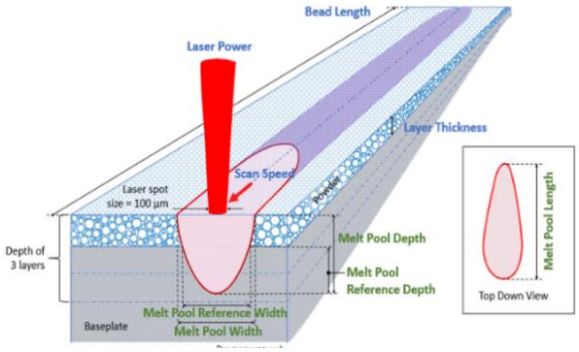

Fig. 1. Schematic illustration containing the base plate, the single beads and their dimensions [2]

The finite element (FE) method is applied to solve the temperature equation (1) by spatial and temporal discretization using initial and boundary conditions stated below:

- The powder bed temperature is fixed at ambient temperature as the initial condition:

$$T=T_0 = 22\ °C = 295\ K \quad (3)$$

- The heat convection Q_c between the powder bed and the surrounding area is defined as follows [11]:

$$Q_c = h\,(T - T_0) \quad (4)$$

where T, h, and T_0 are the temperature, the coefficient of thermal convection, and the initial temperature respectively.

Inconel 718 (IN718) is an excellent superalloy known for its outstanding chemical and mechanical properties at high temperatures. This alloy can be employed at a wide range of high temperatures [4]. In addition, IN718 has a high corrosion resistance. Thanks to these properties, IN718 is used in various industries, such as aeronautic components and gas turbines. However, as far as machinability is concerned, the high mechanical strength of this alloy makes it difficult to use in traditional manufacturing processes. This fact makes it a very popular alloy in additive manufacturing processes. Thus, the IN718 is chosen in our study considering the advantages mentioned above and also for its availability in the materials database of Ansys Additive.

During the process, the thermal properties of the material, including the specific heat, the density and the conductivity, depend on the temperature.

In Ansys Additive, the melt pool is instantaneously tracked along the bead length and then the value of each dimension is averaged over the entire bead length. Data extracted from Ansys Additive are provided Excel files with individual permutations showing the melt pool size for each base plate temperature. The length of the bead is fixed by default 3 mm in Ansys Additive since the melt pool reaches a steady state at this value.

3. RESULTS AND DISCUSSIONS

The predicted melt pool dimensions, including the depth, the width and the length at various base plate temperatures, are analyzed in this section. The figure 3 highlights the effect of the base plate preheating on the depth, width, and length of the melt pool. We notice that both the width and the depth of the melt pool exhibit an increase when the base plate is heated further.

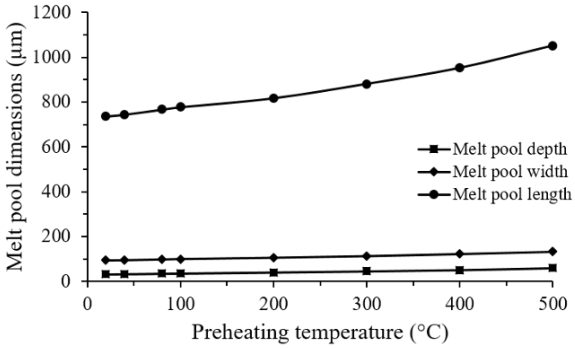

Fig. 3. Melt pool size evolution under various base plate temperatures at P=285 W; V=1500 mm/s

At the same power and scan speed of 285 W and 1500 mm/s, the melt depth becomes about 30% (from 31 µm to 60 µm) deeper and 38% wider (from 94 µm to 132 µm) as the preheating temperature is elevated from 20 °C to 500 °C. We also notice that the increase in width is more pronounced than the one in depth, this suggests that the transfer of energy in the direction of the laser incidence is faster compared to the other directions [26].

Concerning the melt pool length, we notice that the melt pool increases continuously from 737 µm to 1052 µm when varying the base plate temperature from 20°C to 500°C.

Once the laser power is fixed at 285 W (figure 4), and the scan speed is lowered at 500 mm/s, the melt pool width is getting wider about 58% from 193 µm to 251 µm as the preheating temperature varies from 20 °C to 500 °C, which reveals more considerable influence of the preheating temperature on the melt pool width at a slower scan speed.

Concerning the depth, we recorded an increase about 46% (from 152 µm to 251 µm), when the scan speed is 500 mm/s, which shows that the effect of the base plate preheating is more appreciable in comparison with the scan speed 1500 mm/s where the value was 30%.

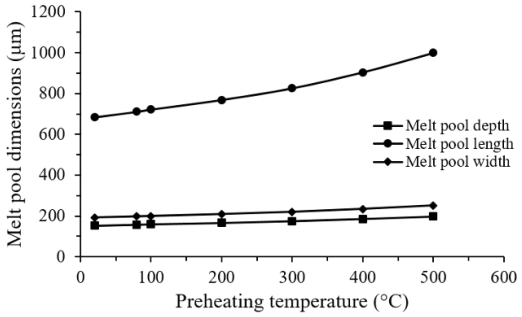

Fig. 4. Dimensions evolution under various base plate temperatures at P=285 W; V=500 mm/s

This implies that the melt pool dimensions become more responsive to the temperature of the base plate at a slower scan speed. Indeed, this finding seems to be obvious since at a slower scanning speed, the time of interaction of the powder bed and the heat source is longer and, thus as a result, the melt pool gets larger and deeper. We wanted to extend our analysis and predict the base plate preheating effects on the degree of porosity development. Figures 5 and 6 outline the level of porosity at various temperatures of preheating.

As it can been seen, the heating of the base plate decreases the degree of porosity which is attributed to the fact that the more the base plate is preheated, the more the solid ratio increases (figure 5) and the void ratio decreases (figure 6), which means a dense solid (solid ratio = 1) without void or pores is obtained (void ratio = 0).

Aiming at validating our numerical results, a comparison with an experimental investigation from literature [5] is carried out. Identical process parameters are adopted in order to ensure that the results are compared on a consistent basis.

The melt pool morphologies extracted from experimental investigations [5] at various base plate preheating temperatures are shown in figure 7.

It is clear that the preheating of the base plate influences significantly the morphology of the melt pool. Raising the base plate temperature enhances the penetration depth of the laser, along with its width, hence, the melt pool volume increases which is in line with our predicted finding where the melt pool dimensions increase with the increase of the base plate temperature.

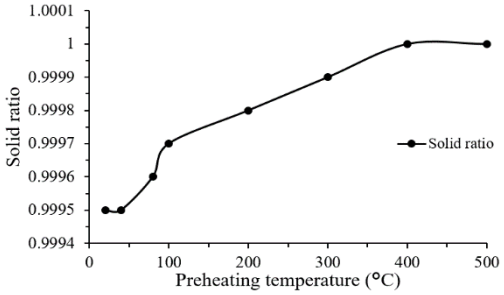

Fig. 5. Solid ratio evolution under various preheating temperatures

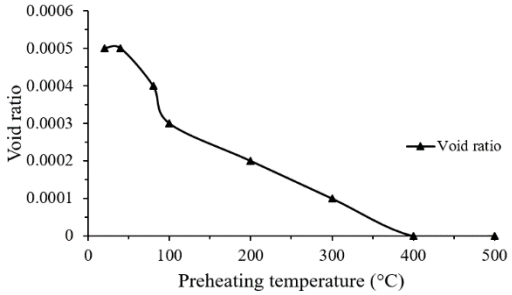

Fig. 6. Void ratio evolution under various preheating temperatures

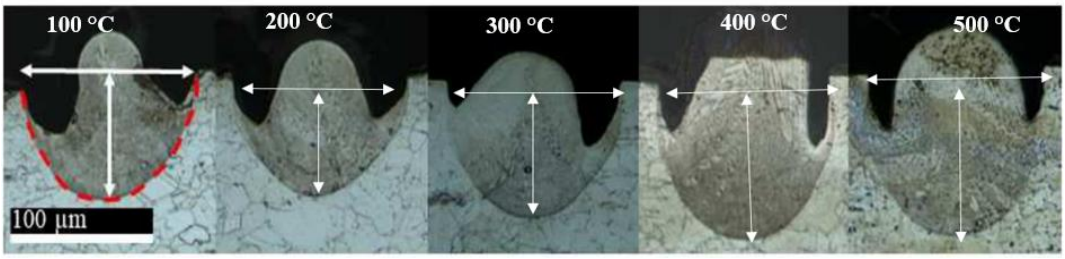

Fig. 7. Morphology of the melt pool under various base plate temperatures [5]

4. CONCLUSIONS

A thermal model based on the finite element method is used to simulate a series of single beads melted on a base plate preheated at various temperatures ranging from 20 °C to 500 °C. During the process the laser power is maintained at the same value, however, the scan speed has been modified from 1500 mm/s to 500 mm/s. Favorable feedback is obtained since the predicted results have proved a considerable dependence between the size of the melt pool and the base plate preheating. In fact, arising the base plate temperature results in a deeper, wider, and longer melt pool. An increase in depth and width by a percentage of 30% and 38% respectively when the scan speed is fixed at 1500 mm/s is reached.

It was also noticed that the preheating condition at 500 °C displayed the prominent impact on the melt

pool size. The melt pool becomes at that temperature wider and deeper when the scan speed is reduced from 1500 mm/s to 500 mm/s, with a percentage of 58% in the width and 46% in the depth indicating that the melt pool is more sensitive to the variation of the base plate temperature at slow scan speed. Altering the base plate temperature indicated the ability to adjust the dimensions of the melt pool. The results may be used as a reference to evaluate the degree of porosity, especially the lack of fusion defect, where the continuous heating of the base plate at high temperatures of 500 °C allows to build a denser solid with limited gaps or pores.

The use of a high base plate temperature was more suitable to prevent void or porosity defects as it guarantees a wide and deep area affected by heat, consequently, voids can be almost filled. The numerical results match fairly with the experimental ones from literature.

We believe that our work may improve knowledge about preheating the base plate and we hope that our numerical methodology will be beneficial in solving the difficulty of experimental trials. Nevertheless, this work can be improved in further study by taking into consideration other building parameters such as the powder layer thickness and the diameter of the laser beam.

REFERENCES

[1]. **Ali H., Ma L., Ghadbeigi H., Mumtaz K.**, *In-situ residual stress reduction, martensitic decomposition and mechanical properties enhancement through high temperature powder bed pre-heating of Selective Laser Melted Ti6Al4V*, Mater. Sci. Eng. A, vol. 695, no. April, pp. 211–220, 2017, doi: 10.1016/j.msea.2017.04.033.

[2]. ***** Ansys,** *Additive User's Guide (Print and Science),* no. January, 2021.

[3]. **Buchbinder D., Meiners W., Pirch N., Wissenbach K., Schrage J.**, *Investigation on reducing distortion by preheating during manufacture of aluminum components using selective laser melting*, J. Laser Appl., vol. 26, no. 1, p. 012004, 2014, doi: 10.2351/1.4828755.

[4]. **Calandri M., Yin S., Aldwell B., Calignano F., Lupoi R., Ugues D.**, *Texture and microstructural features at different length scales in Inconel 718 produced by selective laser melting*, Materials (Basel), vol. 12, no. 8, 2019, doi: 10.3390/ma12081293.

[5]. **Chen Q. et al.**, *Elucidating the effect of preheating temperature on melt pool morphology variation in Inconel 718 laser powder bed fusion via simulation and experiment*, Addit. Manuf., vol. 37, pp. 1–30, 2021, doi: 10.1016/j.addma.2020.101642.

[6]. **Choo H. et al.**, *Effect of laser power on defect, texture, and microstructure of a laser powder bed fusion processed 316L stainless steel*, Mater. Des., vol. 164, Feb. 2019, doi: 10.1016/j.matdes.2018.12.006.

[7]. **Criales L. E., Arısoy Y. M., Lane B., Moylan S., Donmez A., Özel T.**, *Laser powder bed fusion of nickel alloy 625: Experimental investigations of effects of process parameters on melt pool size and shape with spatter analysis*, Int. J. Mach. Tools Manuf., vol. 121, no. September, pp. 22–36, 2017, doi: 10.1016/j.ijmachtools.2017.03.004.

[8]. **Collazo A., Figueroa R., Pérez C. Nóvoa X. R.,** *Effect of Laser Speed and Hatch Spacing on the Corrosion Behavior of 316L Stainless Steel Produced by Selective Laser Melting*, Materials (Basel)., vol. 15, no. 4, 2022, doi: 10.3390/ma15041353.

[9]. **Dong Z., Liu Y., Wen W., Ge J., Liang J.**, *Effect of hatch spacing on melt pool and as-built quality during selective laser melting of stainless steel: Modeling and experimental approaches*, Materials (Basel)., vol. 12, no. 1, Dec. 2018, doi: 10.3390/ma12010050.

[10]. **Hassine N., Chatti S., Ben Slama M., and Kolsi L.**, *Sensitivity of Melt Pool Dimensions and Keyhole To Laser Beam Diameter*, Ann. "Dunarea Jos" Univ. Galati, Fascicle XII, Weld. Equip. Technol., vol. 32, pp. 30–36, 2021, doi: 10.35219/awet.2021.04.

[11]. **Johnson L. et al.**, *Assessing printability maps in additive manufacturing of metal alloys*, Acta Mater., vol. 176, pp. 199–210, Sep. 2019, doi: 10.1016/j.actamat.2019.07.005.

[12]. **Kan W. H. et al.**, *A critical review on the effects of process-induced porosity on the mechanical properties of alloys fabricated by laser powder bed fusion*, J. Mater. Sci., vol. 57, no. 21, pp. 9818–9865, 2022, doi: 10.1007/s10853-022-06990-7.

[13]. **Kantzos C., Pauza J., Cunningham R,. Narra S. P., Beuth J., Rollett A.**, *An investigation of process parameter modifications on additively manufactured inconel 718 parts,* Journal of Materials Engineering and Performance 28(2) (2019) 620-626.

[14]. **Kempen K., Vrancken B., Buls S., Thijs L., Van Humbeeck J., Kruth J. P.**, *Selective Laser Melting of Crack-Free High Density M2 High Speed Steel Parts by Baseplate Preheating*, J. Manuf. Sci. Eng. Trans. ASME, vol. 136, no. 6, pp. 1–7, 2014, doi: 10.1115/1.4028513.

[15]. **Lee Y. S., Zhang W.,** *Modeling of heat transfer, fluid flow and solidification microstructure of nickel-base superalloy fabricated by laser powder bed fusion*, Addit. Manuf., vol. 12, pp. 178–188, 2016, doi: 10.1016/j.addma.2016.05.003.

[16]. **Leicht A., Fischer M., Klement U., Nyborg L., Hryha E.,** *Increasing the Productivity of Laser Powder Bed Fusion for Stainless Steel 316L through Increased Layer Thickness*, J. Mater. Eng. Perform., vol. 30, no. 1, pp. 575–584, 2021, doi: 10.1007/s11665-020-05334-3.

[17]. **Mahamood R. M., Akinlabi S. A., Shatalov M., Akinlabi E. T.**, *Additive manufacturing / 3d printing technology : a review*, Ann. "Dunarea Jos" Univ. Galati, Fascicle XII, Weld. Equip. Technol., vol. 30, pp. 51–58, 2019, doi: 10.35219/awet.2019.04.

[18]. **Malỳ M. et al.**, *Effect of process parameters and high-temperature preheating on residual stress and relative density of Ti6Al4V processed by selective laser melting*, Materials (Basel)., vol. 16, no. 6, 2019, doi: 10.3390/ma12060930.

[19]. **Mirkoohi E., Liang S. Y., Tran H. C., Lo Y. L., Chang Y. C., Lin H. Y.**, *Mechanics modeling of residual stress considering effect of preheating in laser powder bed fusion*, J. Manuf. Mater. Process., vol. 5, no. 2, 2021, doi: 10.3390/jmmp5020046.

[20]. **Plessis A. et al.**, *Effects of process parameters on porosity in laser powder bed fusion revealed by X-ray tomography*, Addit. Manuf., vol. 30, no. September, p. 100871, 2019, doi: 10.1016/j.addma.2019.100871.

[21]. **Qiu C., Panwisawas C., Ward M., Basoalto H. C., Brooks J. W., Attallah M. M.**, *On the role of melt flow into the surface structure and porosity development during selective laser melting* Acta Mater., vol. 96, pp. 72–79, 2015, doi: 10.1016/j.actamat.2015.06.004.

[22]. **Rosenthal Y., Apelstein Y., Rosenthal I., Ashkenazi D., Stern A.**, *On laser powder-bed fusion of additively manufactured alsi10mg alloy: Tensile properties and structure characterization*, Ann. "Dunarea Jos" Univ. Galati, Fascicle XII, Weld. Equip. Technol., vol. 30, pp. 5–12, 2019, doi: 10.35219/awet.2019.01.

[23]. **Tang M., Pistorius P. C., Beuth J. L.**, *Prediction of lack-of-fusion porosity for powder bed fusion*, Addit. Manuf., vol. 14, pp. 39–48, 2017, doi: 10.1016/j.addma.2016.12.001.

[24]. **Tapia G., Elwany A.**, *A Review on Process Monitoring and Control in Metal-Based Additive Manufacturing*, J. Manuf. Sci. Eng. Trans. ASME, vol. 136, no. 6, 2014, doi: 10.1115/1.4028540.

[25]. **Vrancken B., Buls S., Kruth J. P., Humbeeck J. V.**, *Preheating of Selective Laser Melted Ti6Al4V: Microstructure and Mechanical Properties*, 2016.

[26]. **Wang W. et al.**, *Mesoscopic evolution of molten pool during selective laser melting of superalloy Inconel 738 at elevating preheating temperature*, Mater. Des., vol. 213, p. 110355, 2022, doi: 10.1016/j.matdes.2021.110355.

[27]. **Yang Y., van Keulen F., Ayas C.,** *A computationally efficient thermal model for selective laser melting*, Addit. Manuf., vol. 31, p. 100955, 2020, doi: 10.1016/j.addma.2019.